Western North Typhoons with Concentric Eyewalls: 1997-2005 Climatology

H.-C. Kuo
Department of Atmospheric Sciences
National Taiwan University

Chih-Pei Chang
Department of Meteorology
Naval Postgraduate School

H. J. Jiang
Department of Atmospheric Sciences
National Taiwan University

Major issue in intensity change

Black and Willoughby (1992)
Hurricane Gilbert (1988)

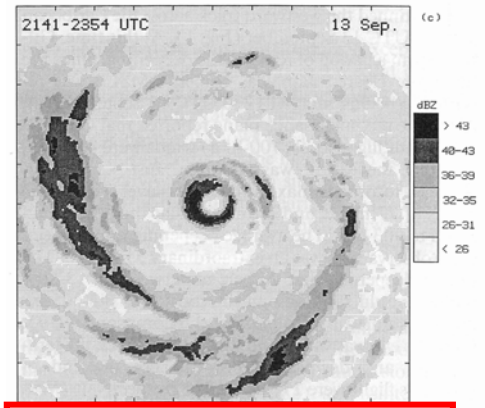

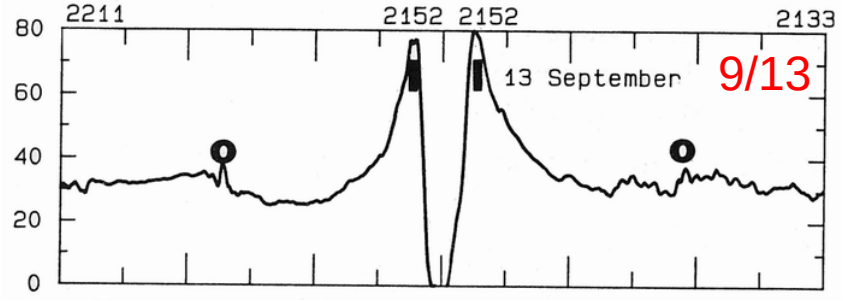

1997-2006

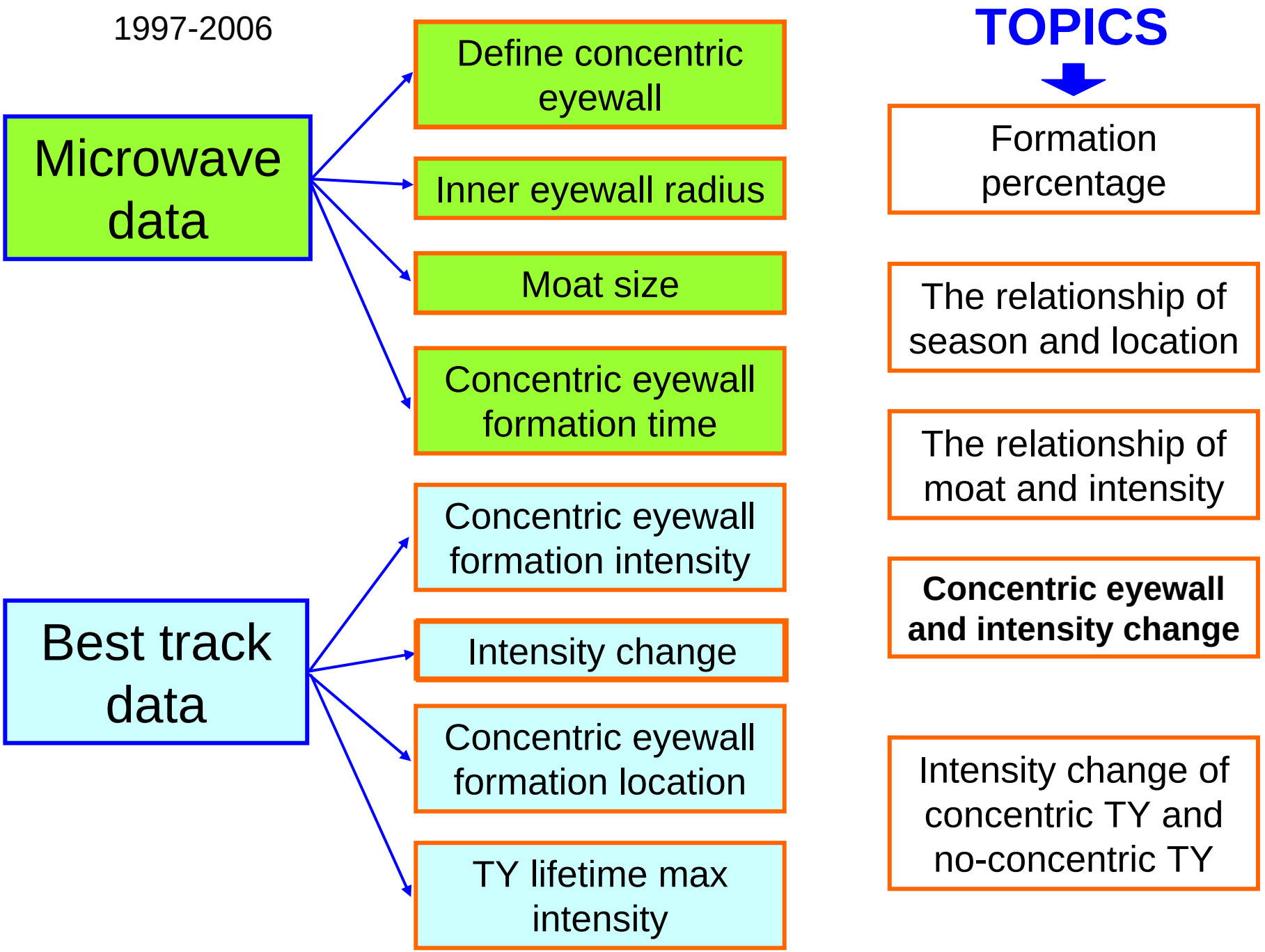
Microwave data
Best track data
Define concentric eyewall
Inner eyewall radius
Moat size
Concentric eyewall formation time
Concentric eyewall formation intensity
Intensity change
Concentric eyewall formation location
TY lifetime max intensity
TOPICS
Formation percentage
The relationship of season and location
The relationship of moat and intensity
Concentric eyewall and intensity change
Intensity change of concentric TY and no-concentric TY

Examples of Concentric Eyewalls

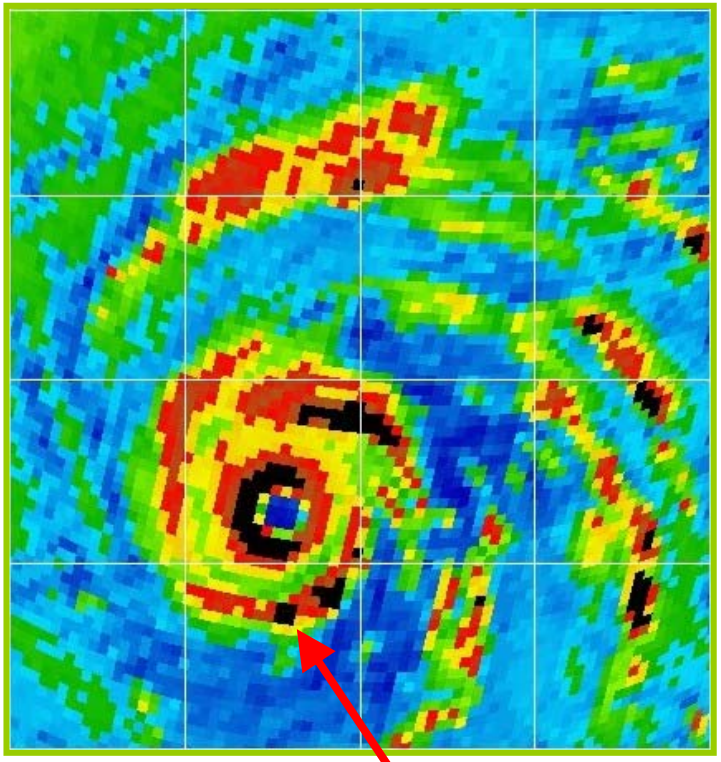

Incomplete outerwall

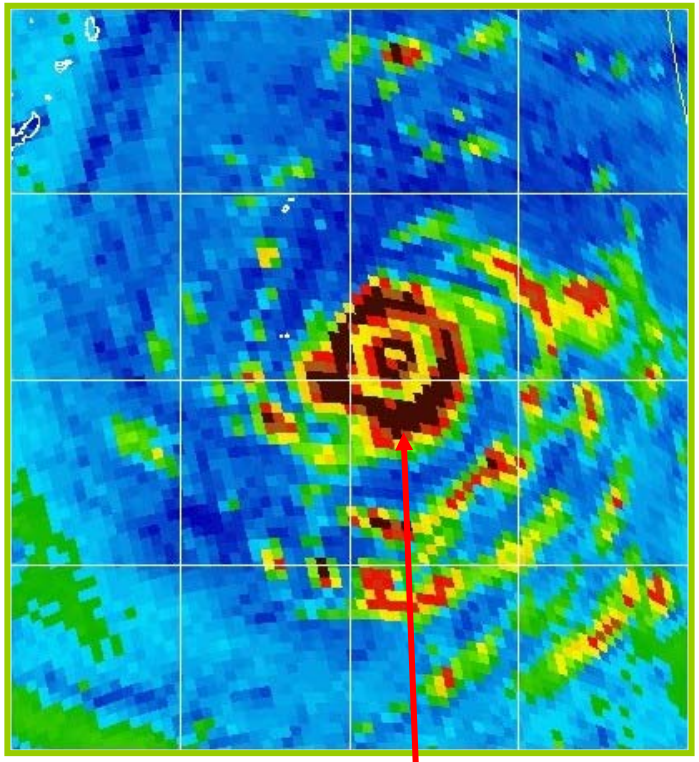

Complete outerwall

≥ 2/3 closed considered complete.

WNPAC Concentric eyewalls formation locations, intensity, and tracks

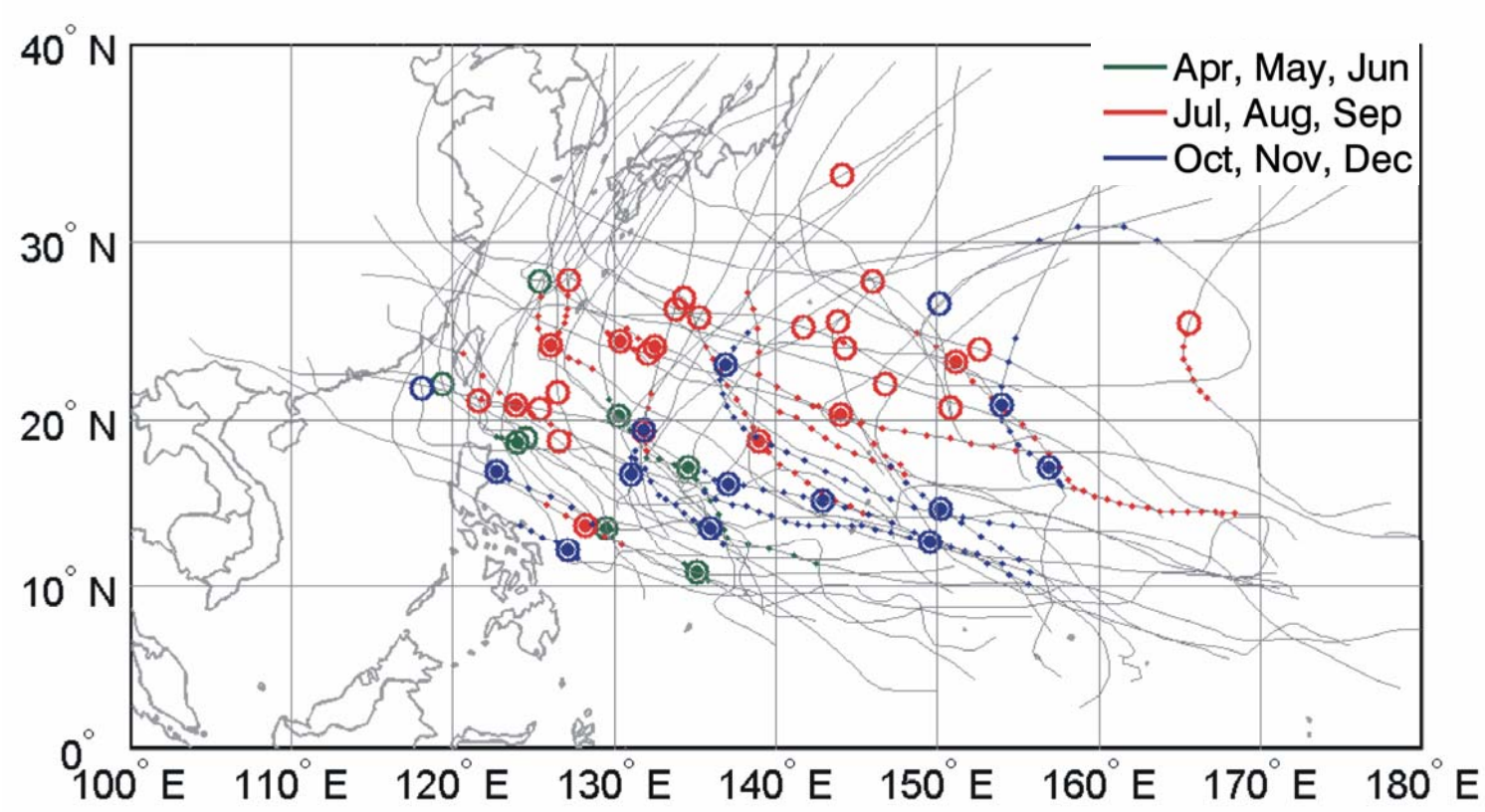

○ : <120 kts

◉ : >120 kts

WNPAC 1997-2005

221 TCs, 205 examined

- 23% formation
- Higher lifetime intensity, higher % of formation

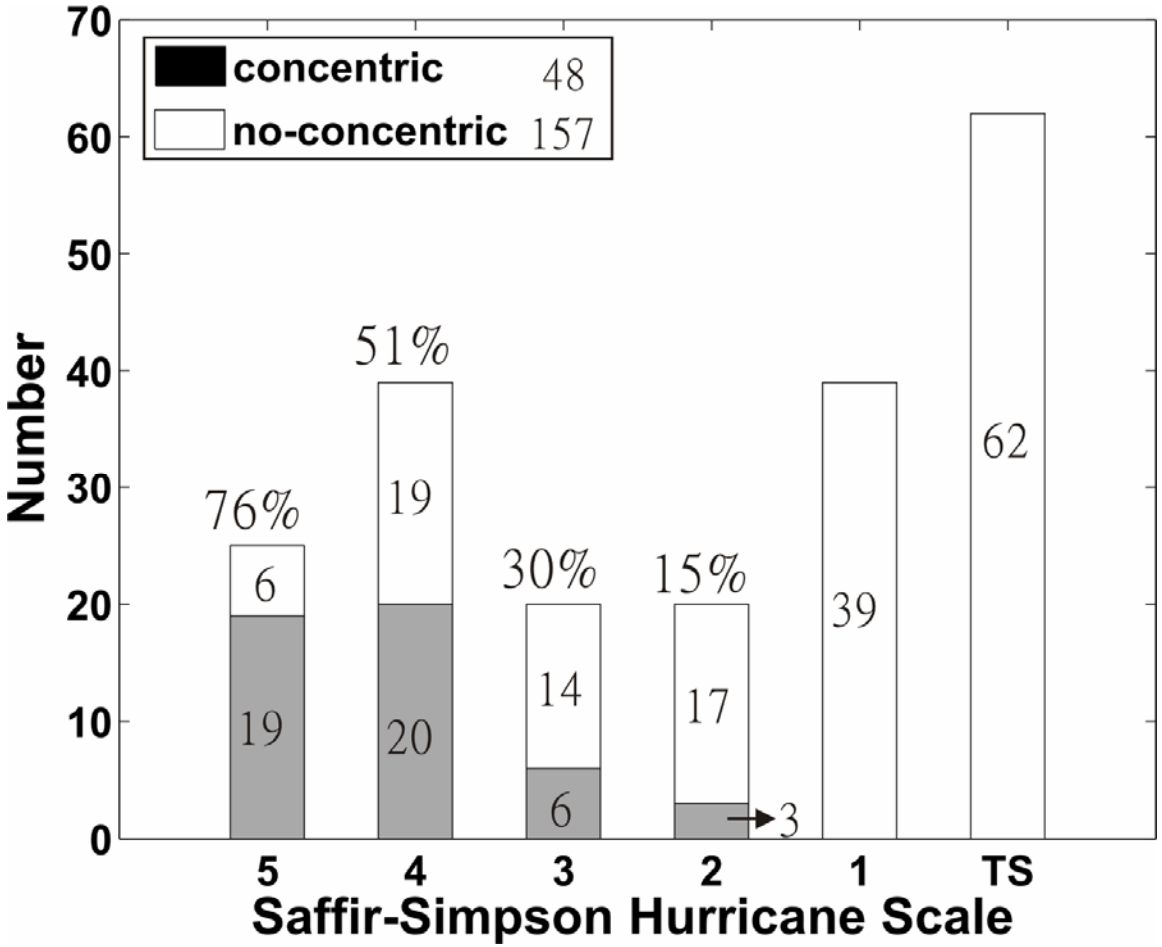

category 5 (135+ kts) category 4 (114-135 kts)

category 3 (96-113 kts) category 2 (83-95 kts)

category 1 (64-82 kts) TS(63- kts)

Intensity at formation time

WNPAC 1997-2005

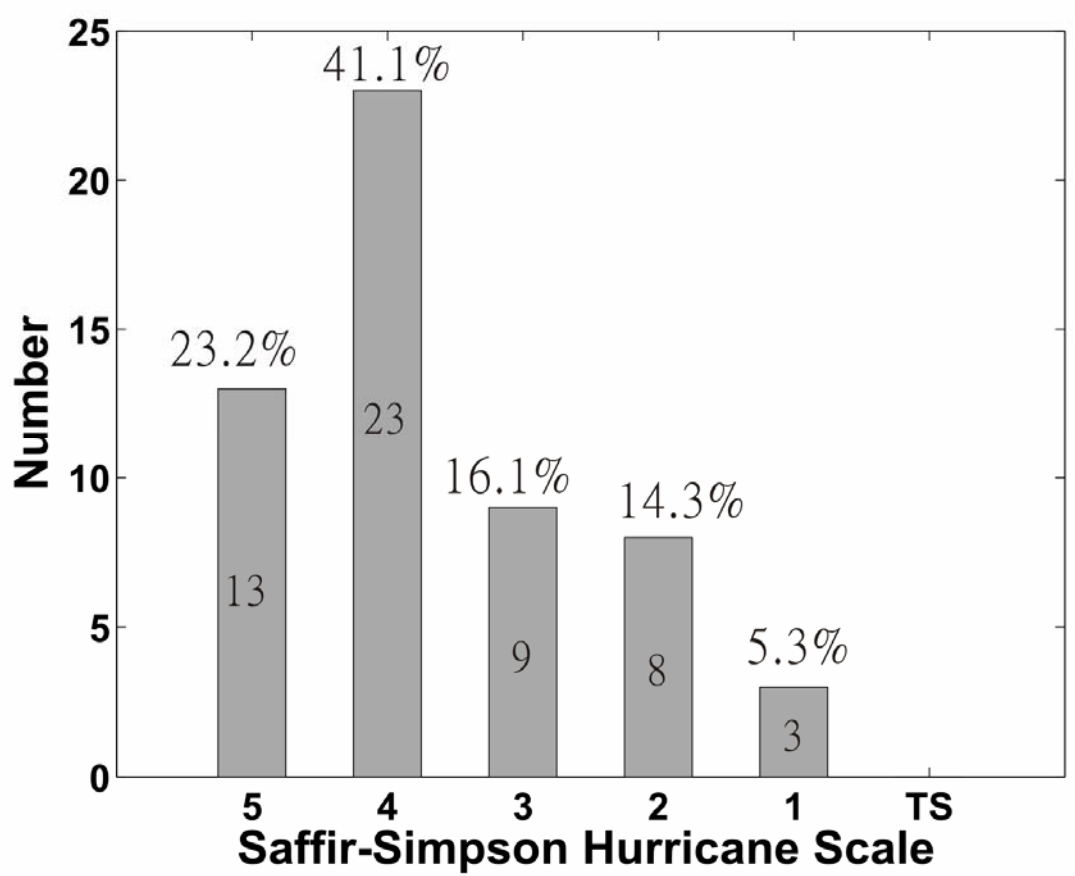

- **64.3% in categories 4 and 5**

Black and Willoughby (1992)

Vertical cross sections of radar reflectivity of the concentric eyewall

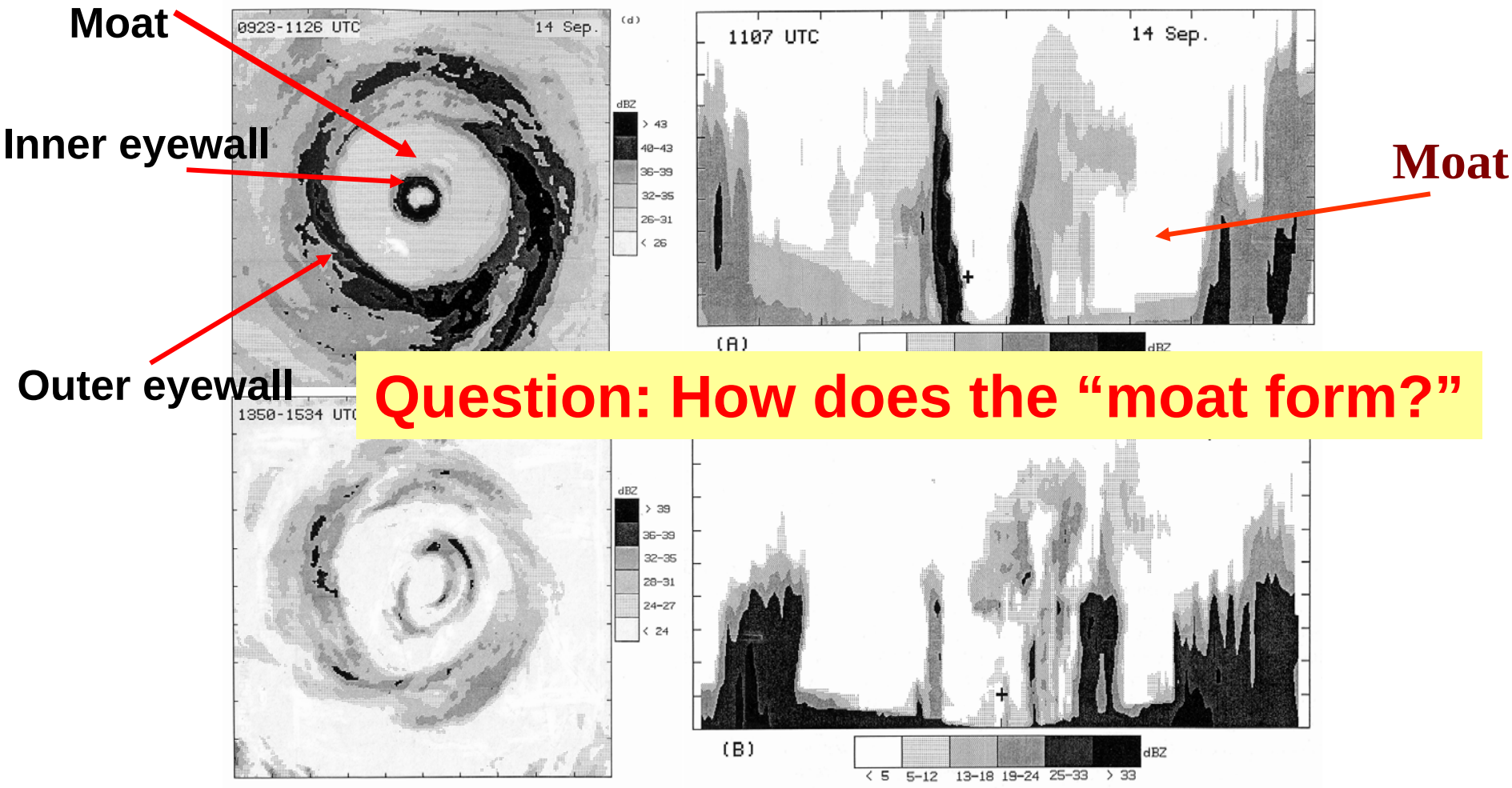

Question: How does the "moat form?"

Thoughts from the 80's and 90's

Moat formation and eyewall replacement are related to the subsidence and the moisture cut-off.

Shapiro and Willoughby (1982) and Schubert and Hack (1982) proposed that heating-vorticity interaction can lead to convective-ring contraction. Stronger, near the TC core favors the inward response.

"Symmetrical Dynamics"

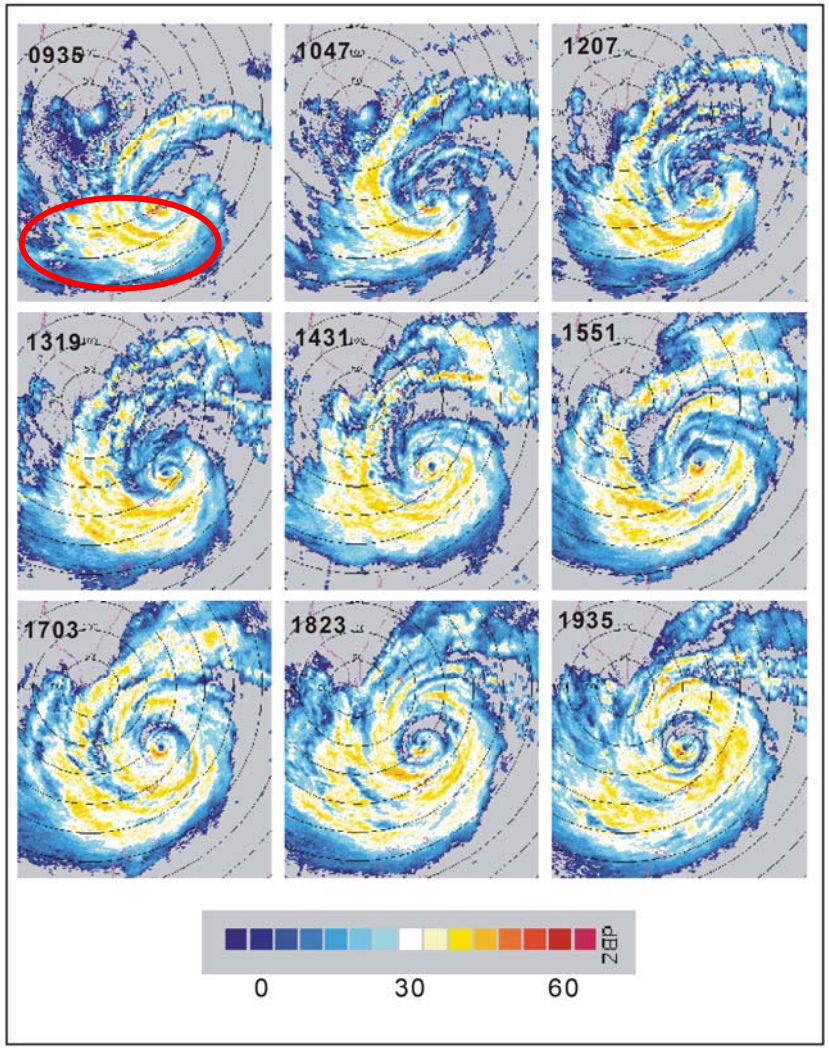

Figure 1a: Reflectivity at 0.5 elevation angle for Typhoon Lekima (2001) from the Central Weather Bureau WSR-88D (10 cm) radar at Kung-Ting for the period 0935 to 1935 September 25. The sequence of the images is from left to right and from top to bottom. The time interval between each image is approximately 75 min. The local time of observation is indicated on top of each image. The radial increment of the circles centered at radar station is 50 km. The nine images illustrate the formation of a concentric eyewalls.

Concentric eyewalls formation in Typhoon Lekima (2001) near Taiwan

Asymmetric Dynamics

Kuo et al. (2004)

Binary vortex interaction.

Dritschel and Waugh's (1992)

$$r = \frac{R_1}{R_2}$$

$$\Delta / R_1$$

Kuo et al. (2004) $\gamma = \frac{\zeta_1}{\zeta_2}$

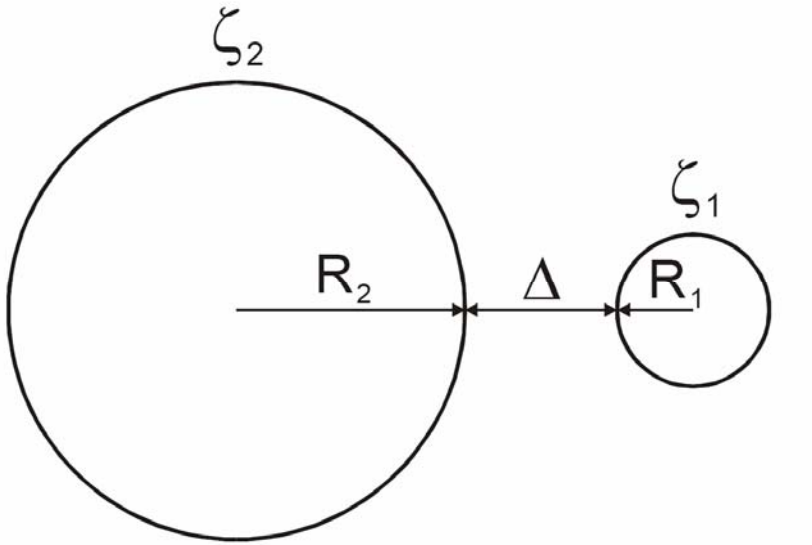

Interaction of:
1. a small and strong vortex (representing TC core) with
2. a large and weak vortex (representing vorticity induced by convection outside the TC core)

$$\gamma = \frac{\zeta_1}{\zeta_2}$$

Kuo et al. (2004)

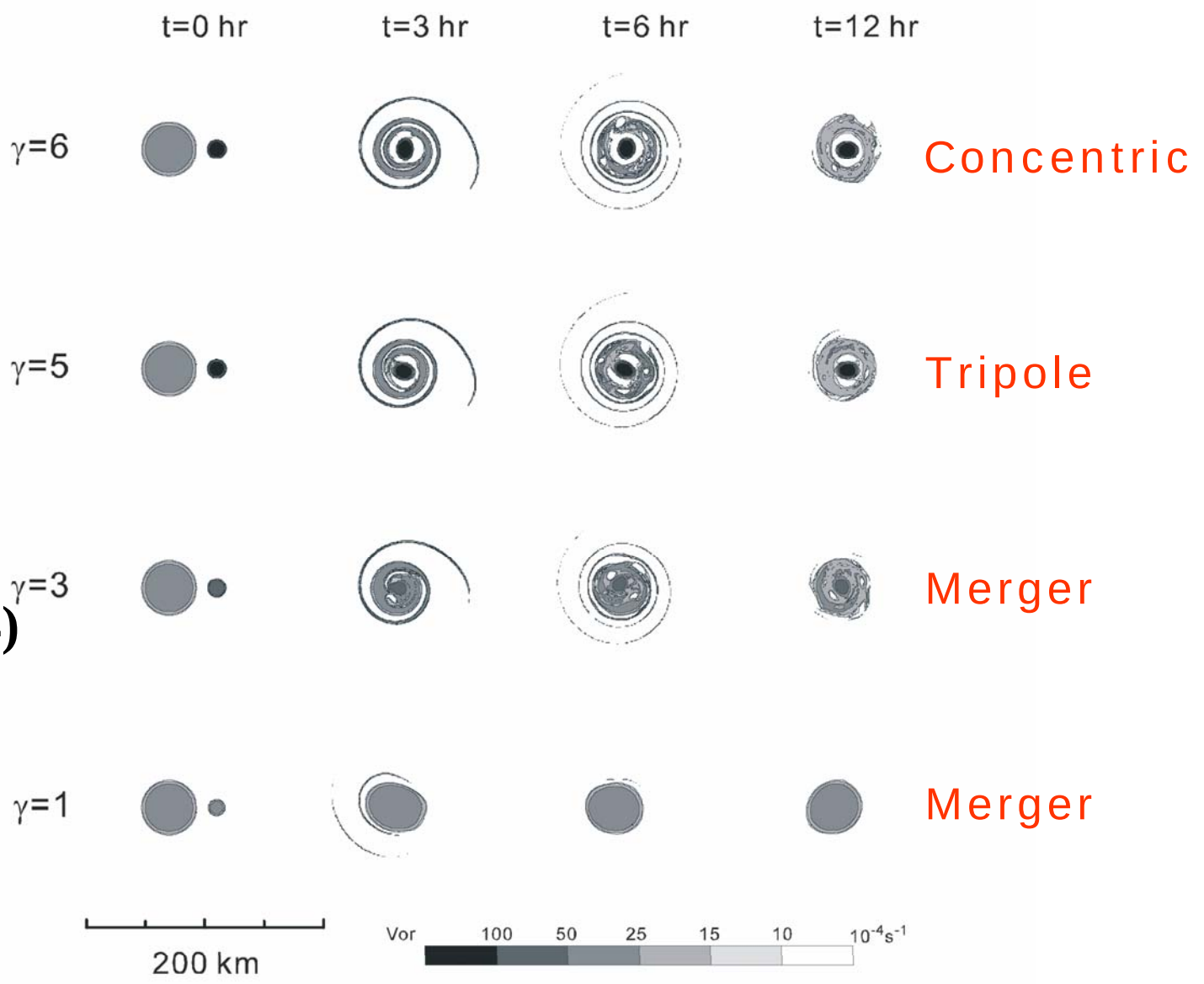

Figure 3: The sensitivity of the vorticity field in the binary vortex experiments with respect to the vorticity strength ratio (γ) at hour 0, 3, 6 and 12 with the dimensionless gap $\Delta/R_1=1$, and the vortex radius ratio r=1/3.

Moat width v.s. Core size

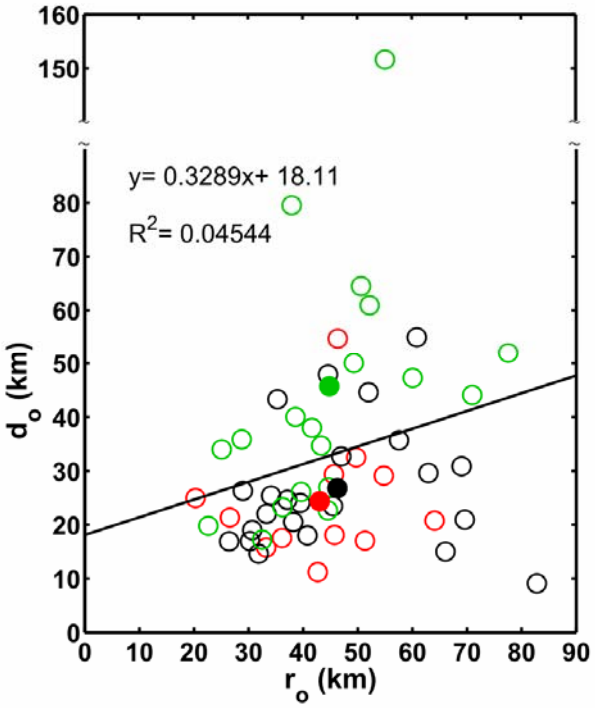

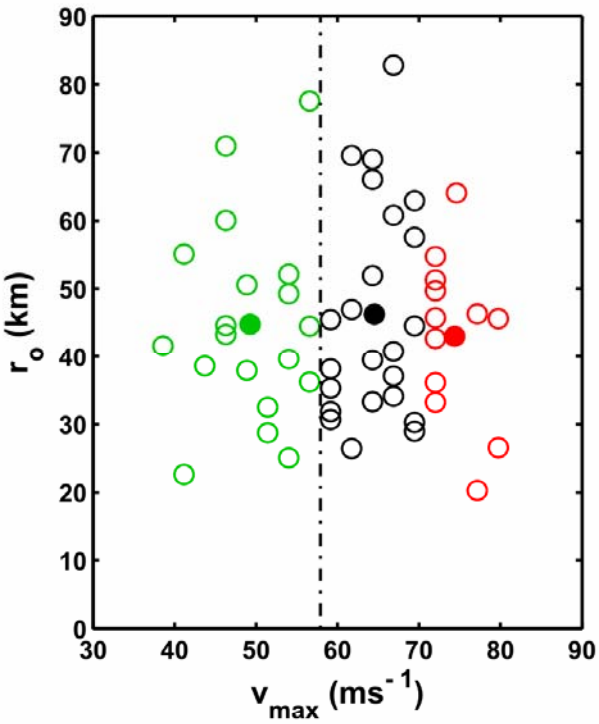

Core size v.s. Intensity

Moat width v.s. Core vorticity

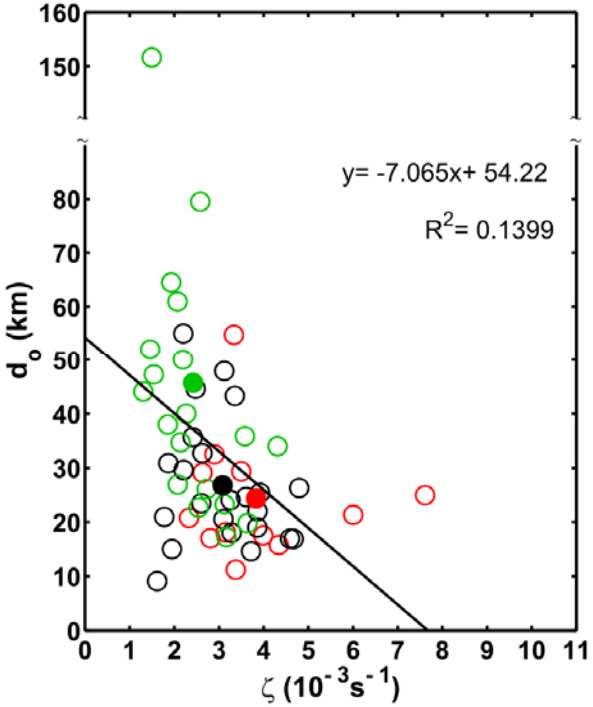

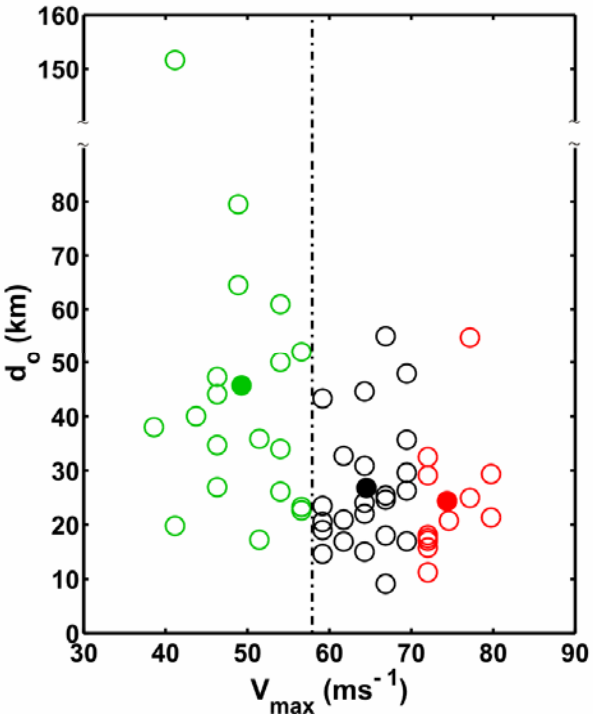

Moat width v.s. Intensity

Rozoff et al. (2006)

The strong differential rotation outside RMW.

filamentation time $\leq$ 30 min (convective turnover time).

"Rapid Filamentation Zone"

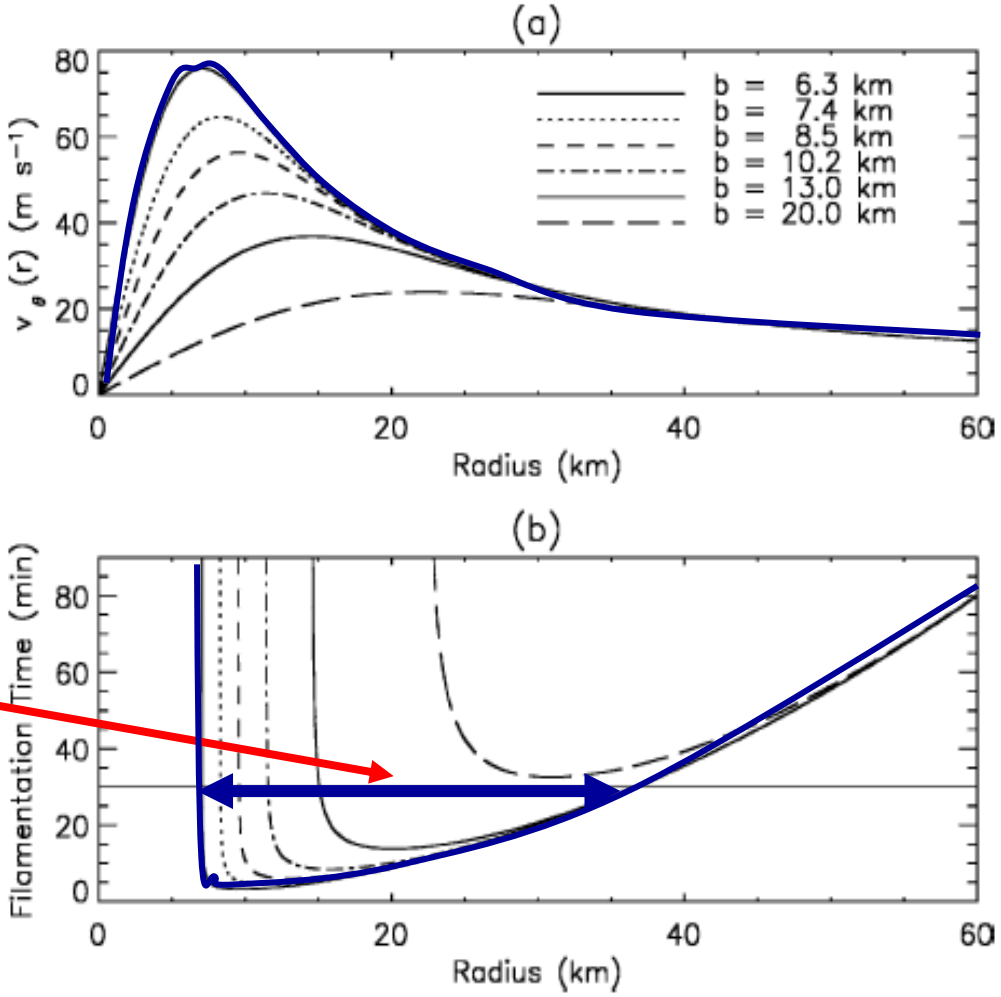

FIG. 2. (a) Radial profiles of v_θ (r) as given by (15) for six different values of the parameter b. (b) Corresponding radial profiles of $\tau_{\text{fil}}(r)$ as given by (16). The filamentation times $\tau_{\text{fil}}(r)$ are plotted only in the strain-dominated regions, where $S_1^2 + S_2^2 - \zeta^2 > 0$.

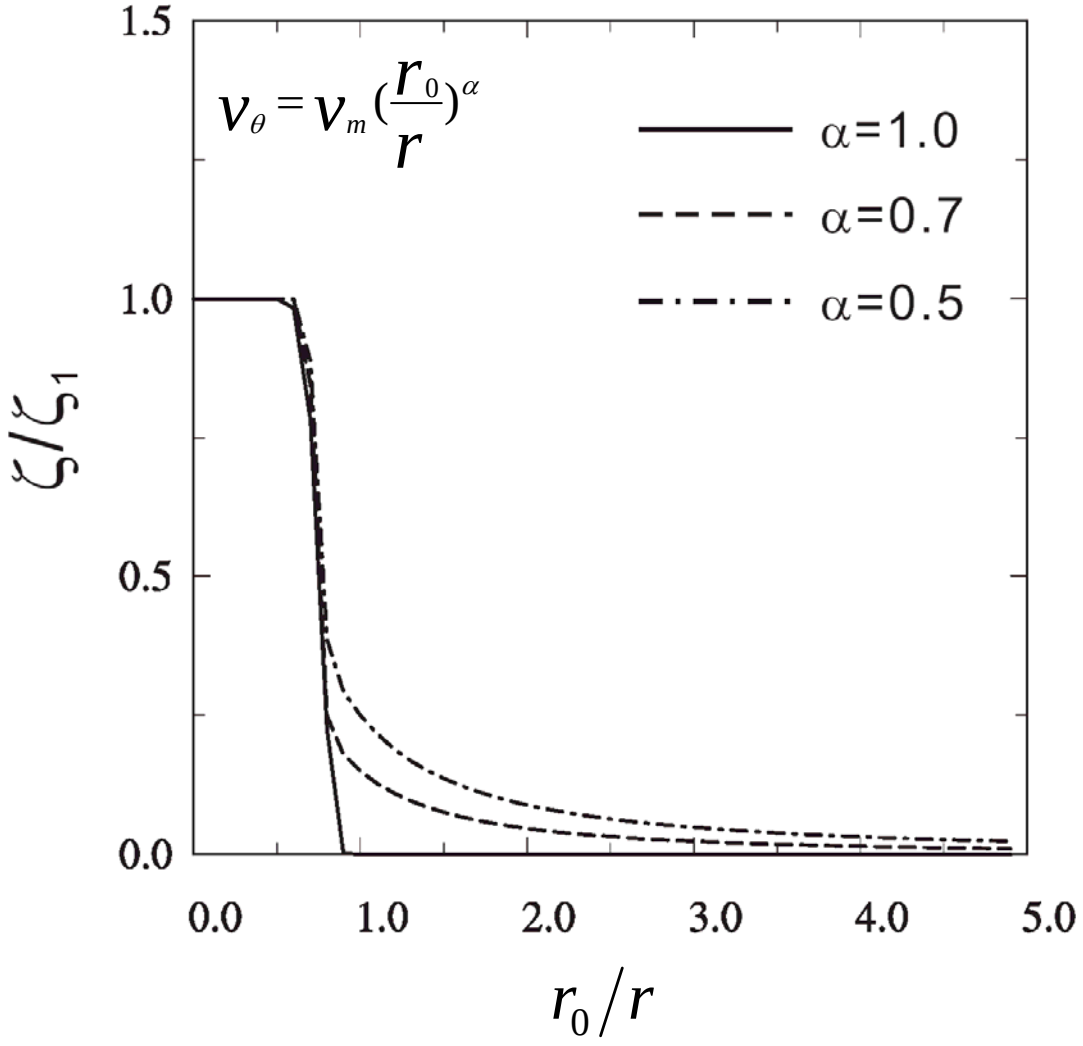

Skirt of significant relative vorticity: slow decrease of v_θ outside RMW (Mallen et al. 2005)

Radial profile of the vorticity for the core vortex with the skirt parameter (α) 1.0, 0.7 and 0.5.

Moat size (d_{ft}) estimated from filamentation time

$$\tau_{fil} = 2 \Big/ \sqrt{\left(\frac{\partial v_\theta}{\partial r} - \frac{v_\theta}{r}\right)^2 - \left(\frac{\partial v_\theta}{\partial r} + \frac{v_\theta}{r}\right)^2}$$

$$\tau_{fil} = \frac{r}{v_\theta \sqrt{\alpha}} = \boxed{\frac{2}{\zeta}\left(\frac{r}{r_0}\right)^{\alpha+1} \alpha^{-\frac{1}{2}} = \tau_0}$$

$$\frac{r}{r_0} = \left(\frac{\zeta}{2} \tau_0 \alpha^{\frac{1}{2}}\right)^{\frac{1}{\alpha+1}}$$

$$\boxed{d_{ft} = r - r_0 = \left(\frac{\zeta}{2} \tau_0 \alpha^{\frac{1}{2}}\right)^{\frac{1}{\alpha+1}} r_0 - r_0}$$

v_m : best track data

r_0 : inner eyewall radius

$$v_\theta = v_m \left(\frac{r_0}{r}\right)^\alpha$$

$$\zeta = 2 \frac{v_m}{r_0}$$

$$\tau_0 = 30 \text{ min}$$

Nondimensional moat width v.s. nondimensional filamentation moat width

All cases

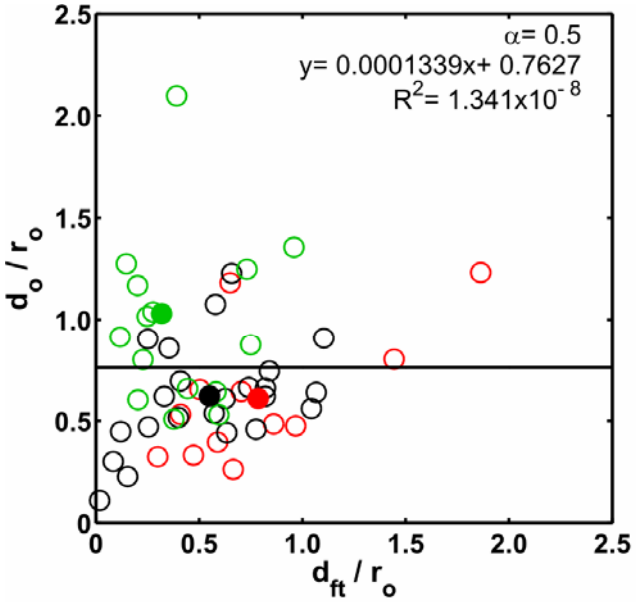

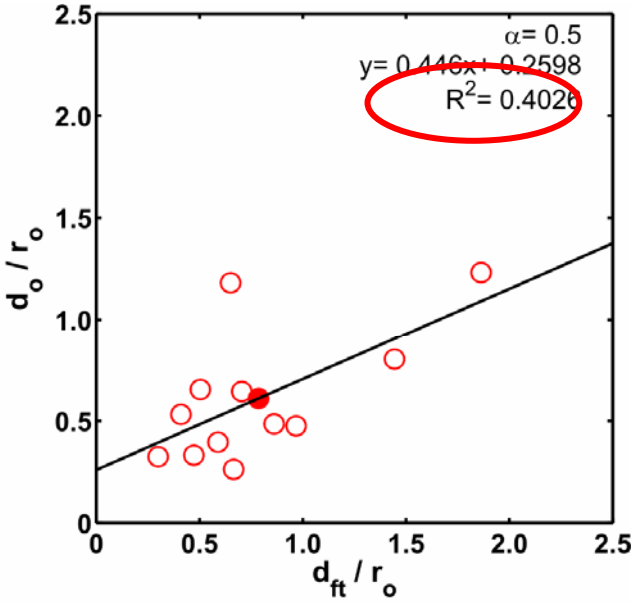

Cat 5

Cat 4

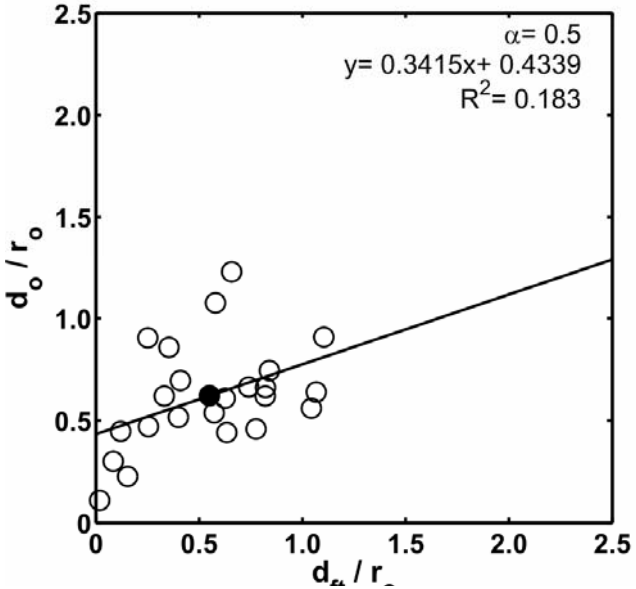

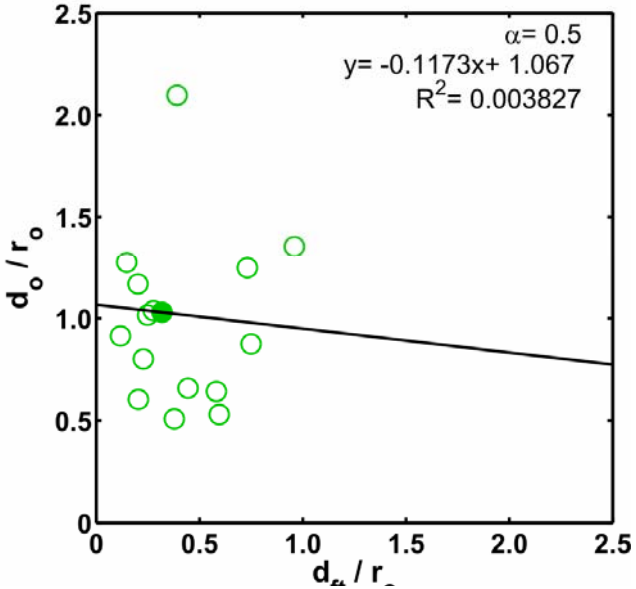

Cat 3

Nondimensional moat width v.s. nondimensional filamentation moat width

All cases

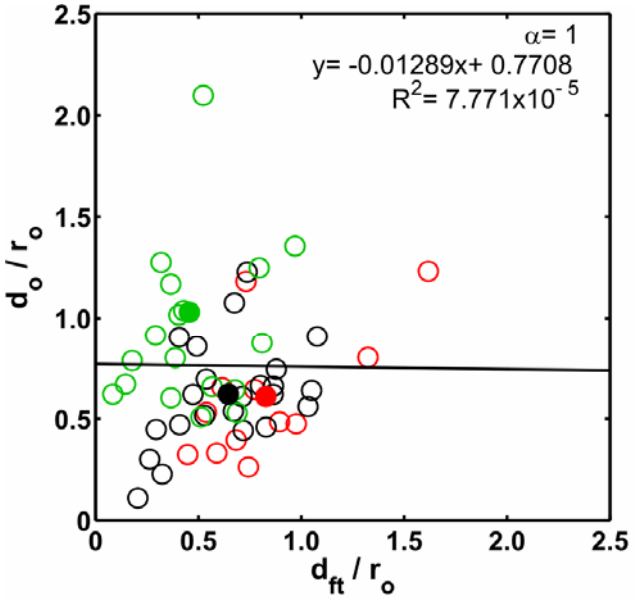

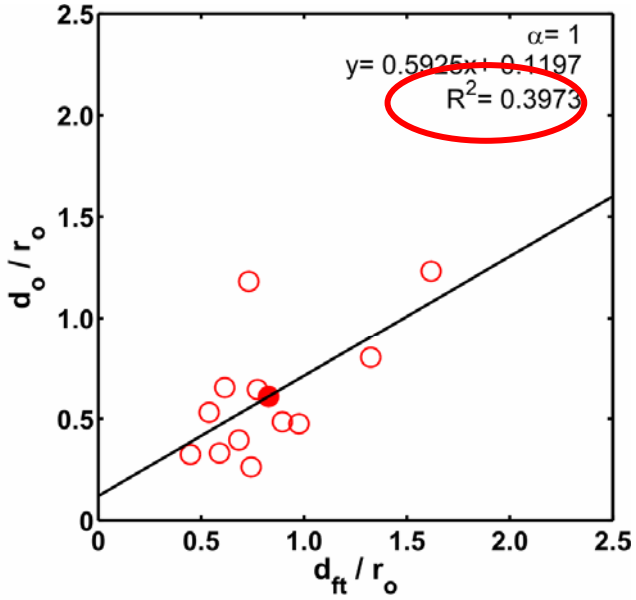

Cat 5

Cat 4

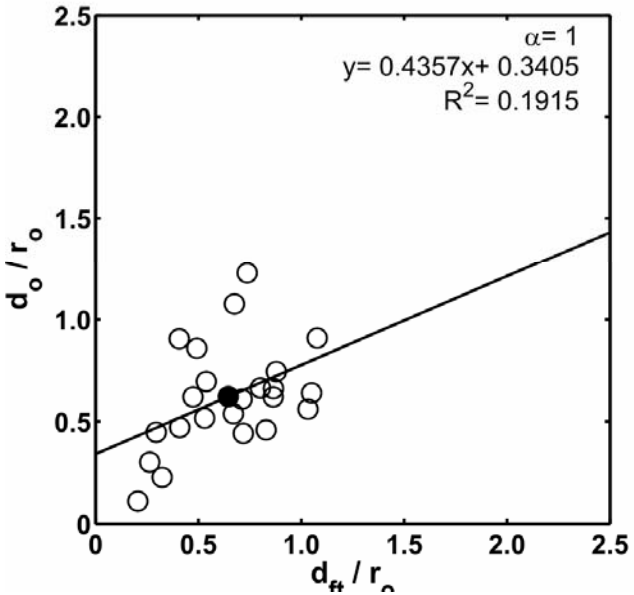

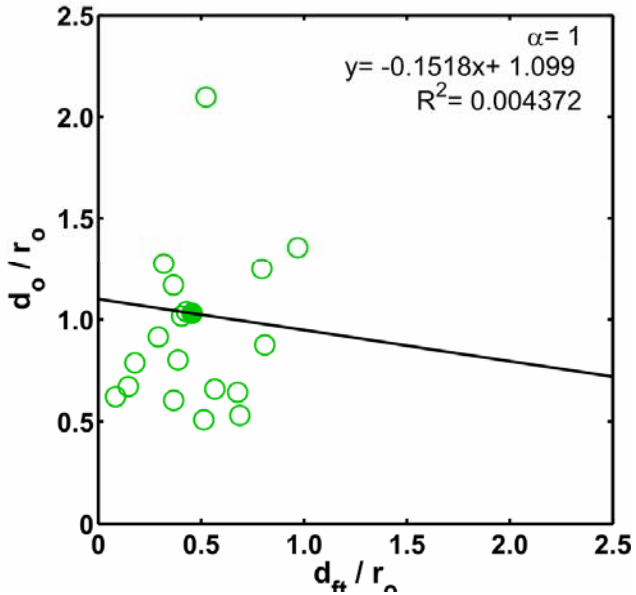

Cat 3

Intensity change 24h before and after the formation of concentric eyewalls

+:intensity increase (P) - : intensity decrease (N)

+-

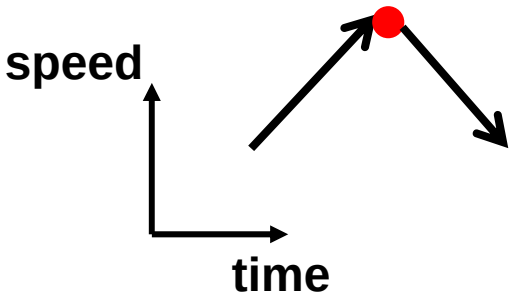

--

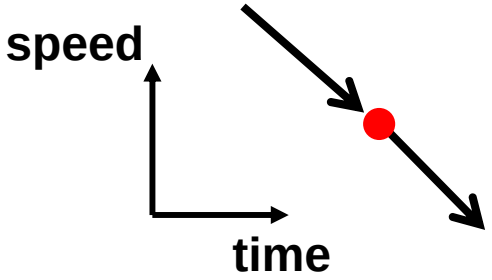

++

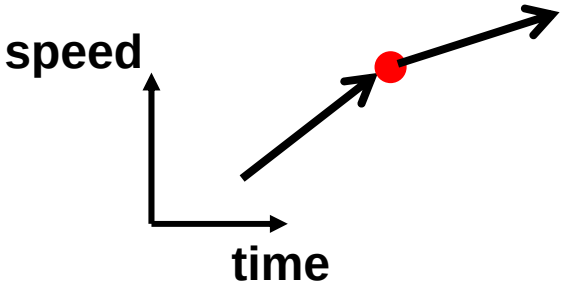

-+

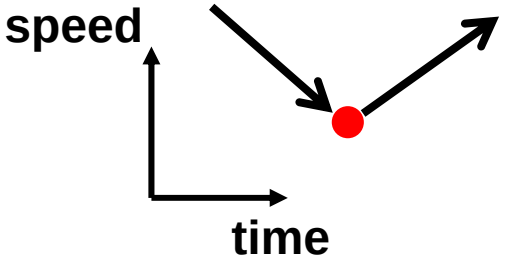

1997 Paka
Type:PN

concentric

121406Z-64m/s
1214-0835Z

121506Z-72 m/s
1215-0822Z

121606Z-64 m/s
1216-0721Z

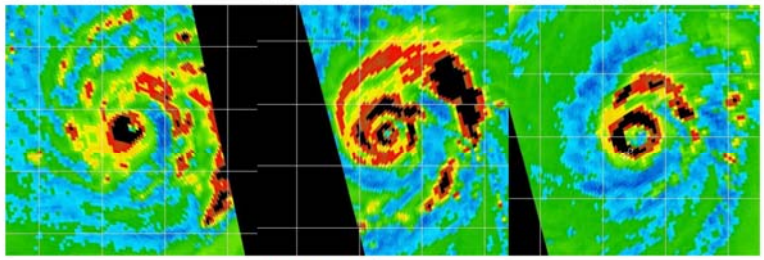

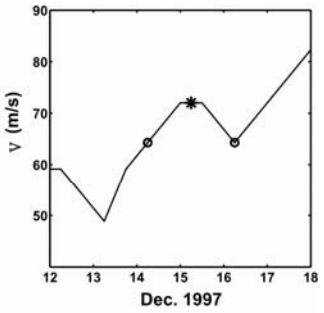

PN
+-

1997 Amber
Type:PP

concentric

082600Z-44 m/s
0826-0135Z

082618Z-49 m/s
0826-2054Z

082712Z-57 m/s
0827-1337Z

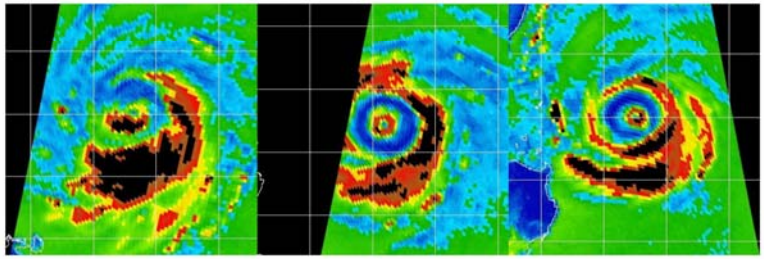

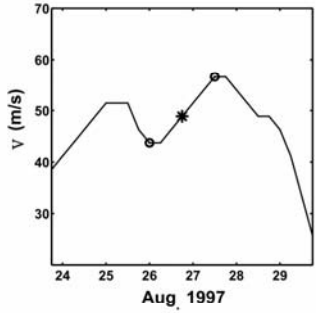

PP
++

1997 Winnie
Type:NN

concentric

081500Z-54 m/s
0814-2316Z

081600Z-44 m/s
0816-0154Z

081700Z-39 m/s
0816-2114Z

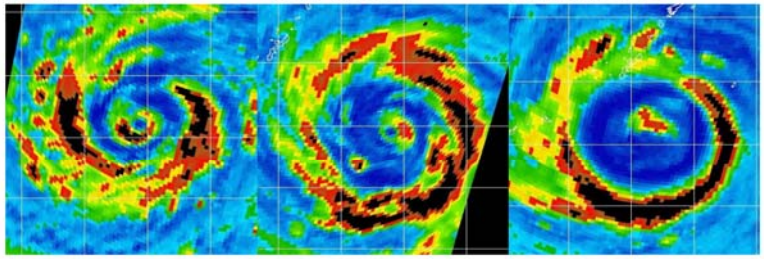

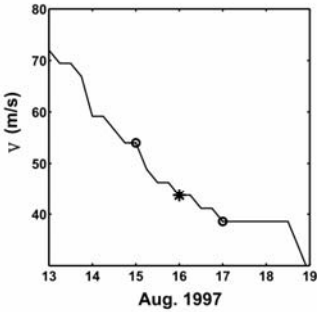

NN
--

2004 Chaba
Type:NP

concentric

082612Z-59 m/s
0826-1012Z

082712Z-54 m/s
0827-0920Z

082812Z-57 m/s
0828-0906Z

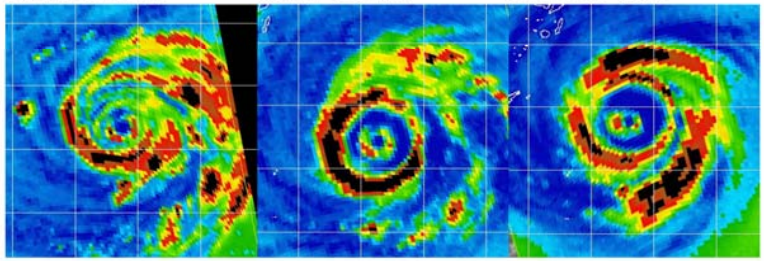

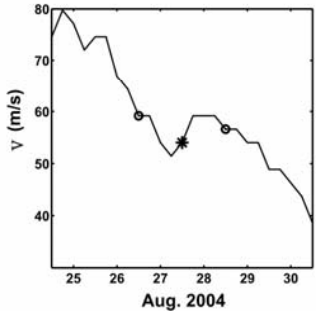

NP
-+

Composite time series of the intensity for the NP, NN, PN, and PP cases

➢**74%** (PN+PP) cases intensity increase 24h before concentric eyewalls formation

➢**72%** (PN+NN) cases intensity decrease 24h after the concentric eyewalls formation

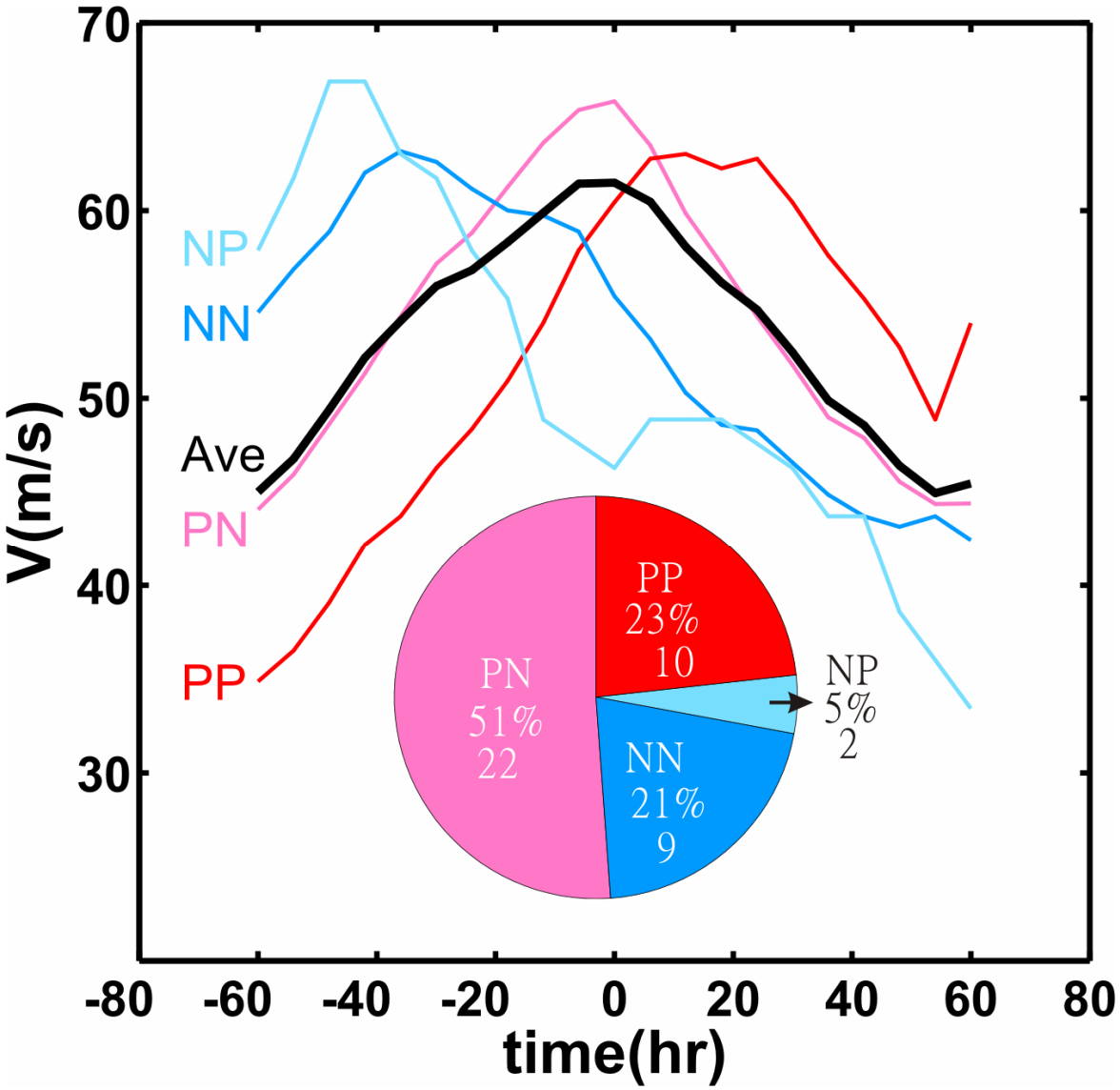

Knaff and Koss

- color-enhanced IR image of Hurricane Luis (1995) at 2015 UTC 3 Sep

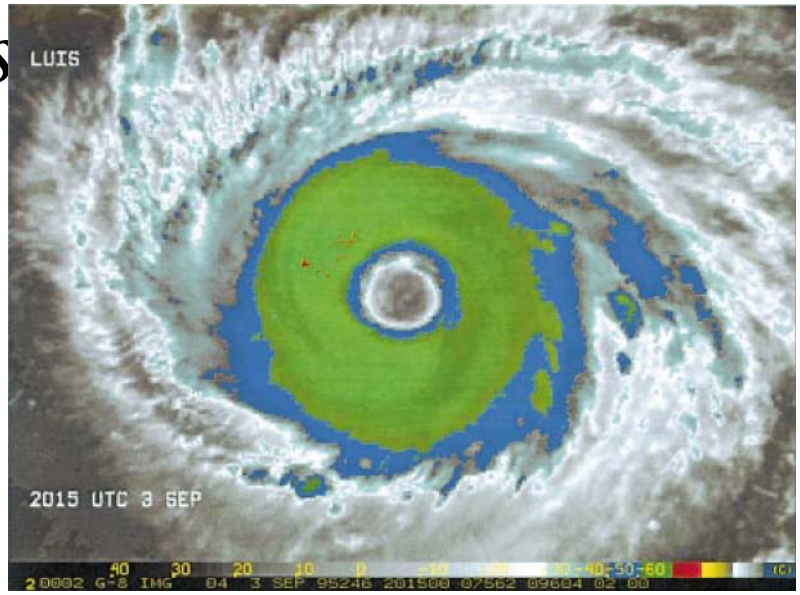

dimensionless	24-h weakening
ATL(56)	0.14
Annular hurricanes(6)	0.05

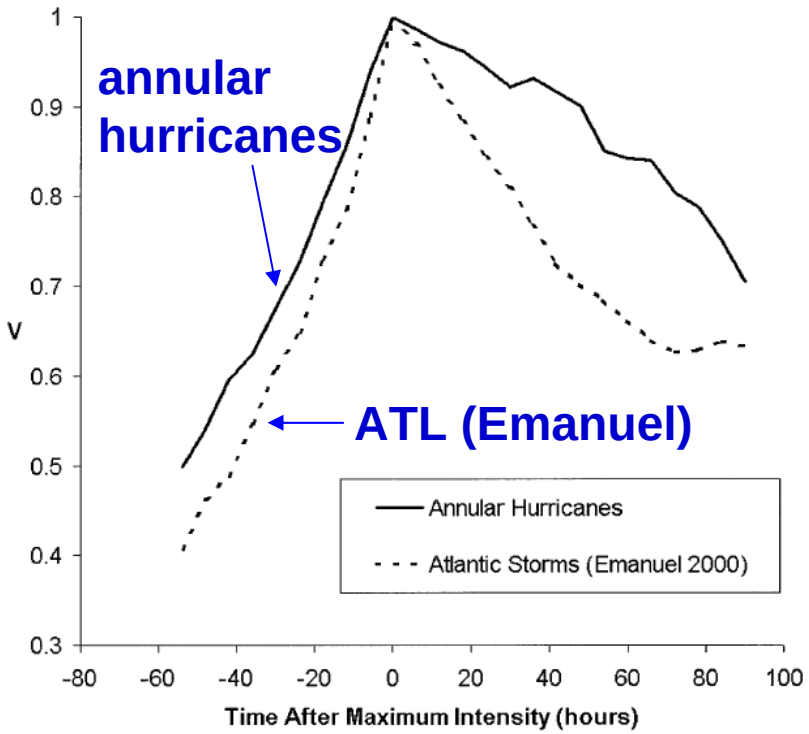

Composite time series of intensity for concentric and non-concentric cases

Cat 4 and 5

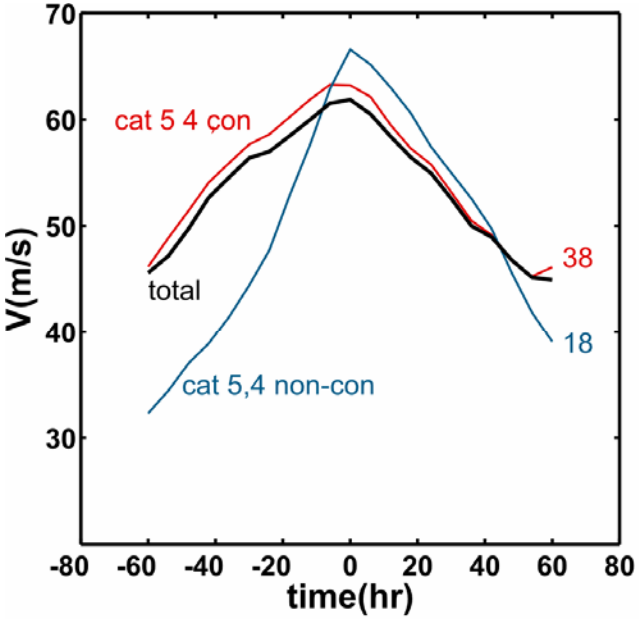

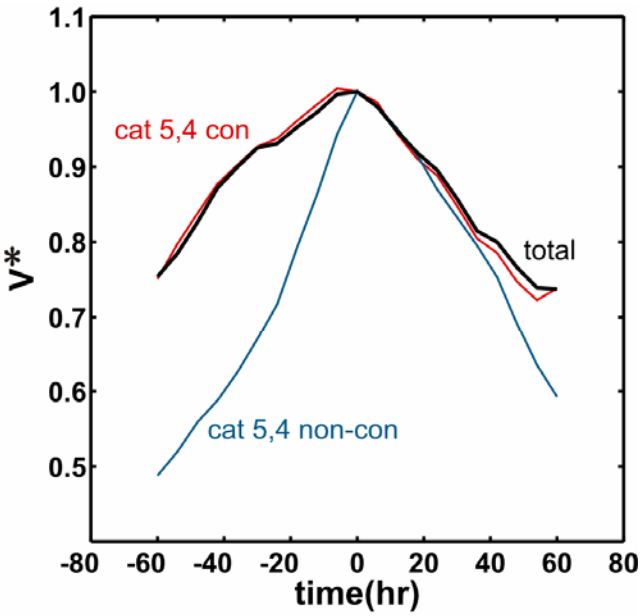

Cat 2 and 3

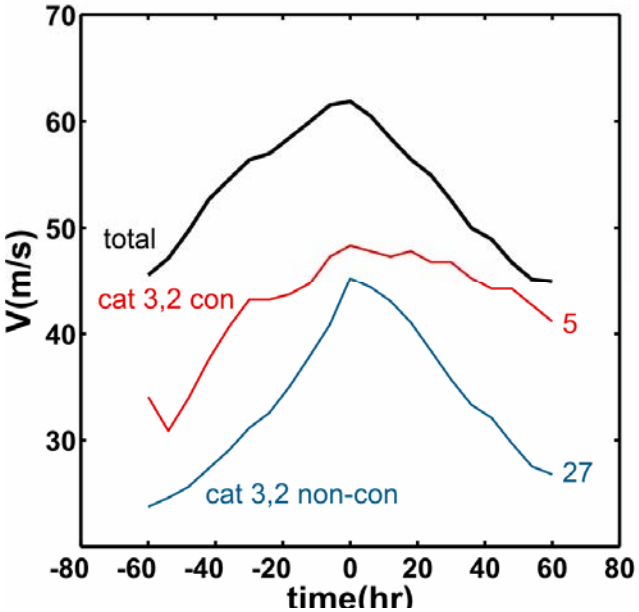

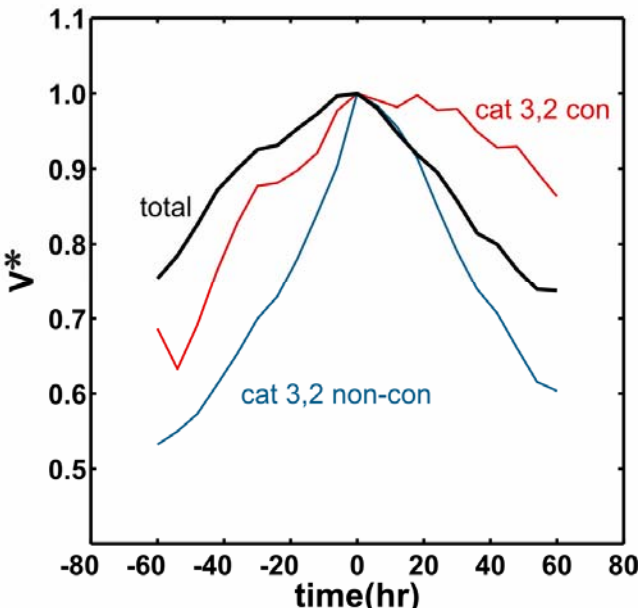

Composite Time Series of the Normalized Intensity

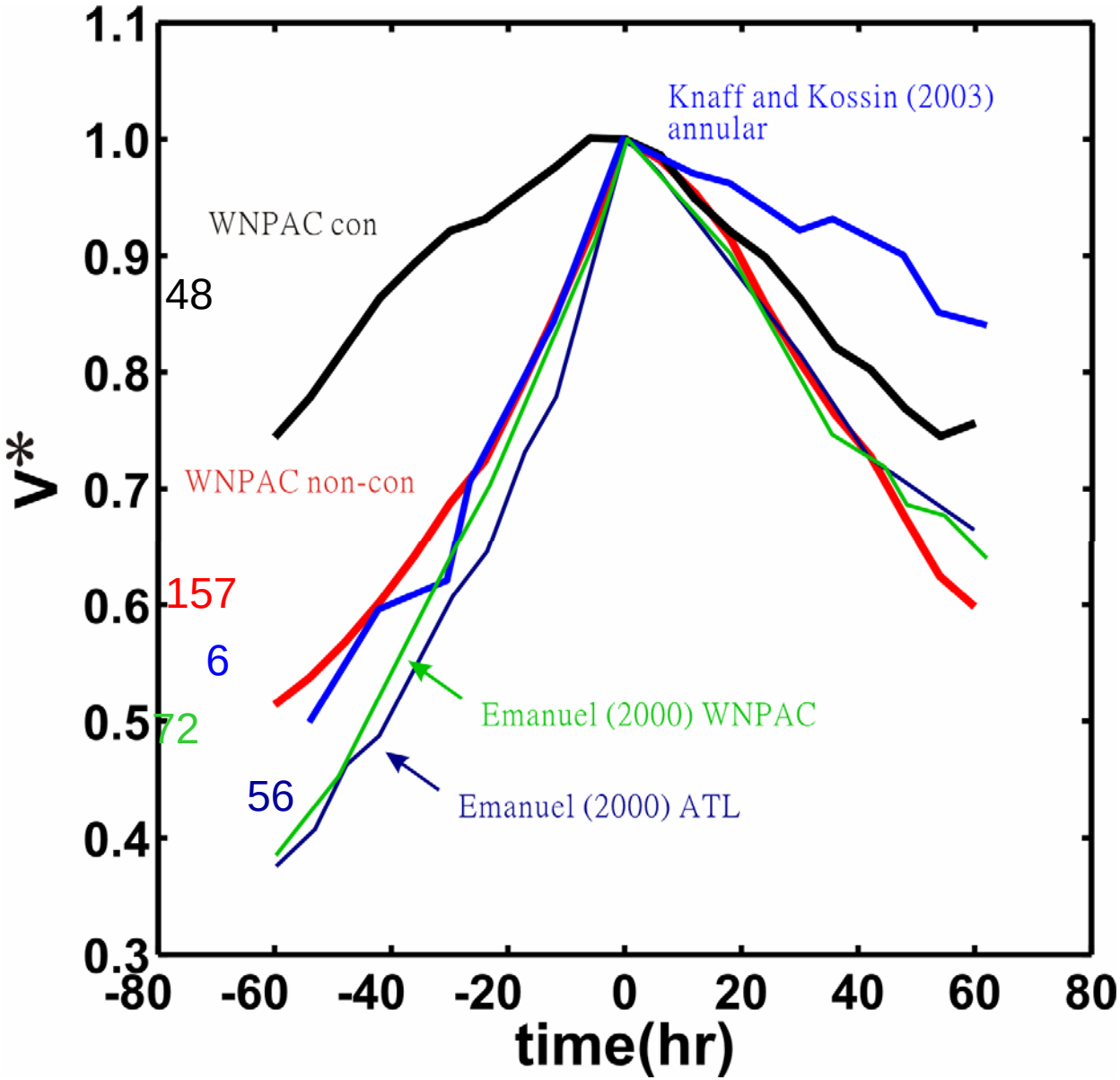

Summary

1. Formation occurred in 23% of WNPAC TCs :
   - 64% of formation occurred in categories 4 and 5.
   - 51% of category 4 and 76% of category 5 possessed it.

2. Higher latitude formation (>25N) occurs at lower intensity (<120 knots).

3. Core size, intensity, core vorticity, and moat width are all little related.

4. The mechanism of moat formation through rapid filamentation dynamics is important in strong typhoons.

- The “filamentation moat size” explains 40% of the of the satellite observed variance for category 5 typhoons.

5. Intensity of the concentric eyewall typhoons tends to peak at the time of concentric eyewalls formation.

- Approximately 74% cases intensify 24h before concentric formation and approximately 72% cases weaken 24h after formation.

6. Formation depends on the maintenance of a relatively high intensity for a longer duration, rather than a rapid intensification process that can reach a higher intensity. (No difference in the weakening phase.)

Thank you